Postprint of: Pietrenko-Dabrowska A., Koziel S., Accelerated design optimization of miniaturized microwave passives by design reusing and Kriging interpolation surrogates, AEU - International Journal of Electronics and Communications, Vol. 118 (2020), 153165, DOI: 10.1016/j.aeue.2020.153165

Accelerated Design Optimization of Miniaturized Microwave Passives by Design Reusing and Kriging Interpolation Surrogates

Anna Pietrenko-Dabrowska[1] and Slawomir Koziel[2,1]

[1] Faculty of Electronics, Telecommunications and Informatics, Gdansk University of Technology, 80-233 Gdansk, Poland, anna.dabrowska@pg.edu.pl

[2] Engineering Optimization & Modeling Center, Reykjavik University, 101 Reykjavik, Iceland, koziel@ru.is,

Corresponding author: anna.dabrowska@pg.edu.pl

Keywords: Microwave design, design optimization, EM-driven design, surrogate modeling, metamodeling, kriging interpolation.

Abstract

Electromagnetic (EM) analysis has become ubiquitous in the design of microwave components and systems. One of the reasons is the increasing topological complexity of the circuits. Their reliable evaluation—at least at the design closure stage—can no longer be carried out using analytical or equivalent network representations. This is especially pertinent to miniaturized structures, where considerable EM cross-coupling effects occurring in densely arranged layouts affect the performance in a non-negligible manner. Although mandatory, EM-driven design is normally associated with significant computational expenses. Consequently, expediting the procedures that require massive simulations, such as parametric optimization, is a practical necessity. In this paper, a framework for accelerated parameter tuning is proposed. The keystones of our methodology are a set of pre-existing designs optimized for various design objectives, as well as kriging interpolation surrogates. The latter are constructed to yield—for a given set of performance specifications—a reasonably good starting point and to enable rapid optimization by providing the initial approximation of the Jacobian matrix of the circuit outputs. The proposed approach is validated using two compact impedance matching transformers designed within the objective spaces defined by wide ranges of operating bandwidths. As demonstrated, the average tuning cost corresponds to a few EM simulations of the respective circuit despite large numbers of adjustable parameters.

1. Introduction

It is a fact of the matter that full-wave electromagnetic (EM) simulation tools have become deeply rooted in the realm of microwave design [1]-[3]. While, in many cases, the initial designs can still be obtained through analytical considerations or from equivalent network models, it is virtually imperative for the majority of modern structures that the design closure (final adjustment of geometry parameters) is conducted at the level of EM models [4]-[6]. Miniaturized microwave components (couplers, power dividers, filters) belong to representative examples of circuits where EM-driven design is necessary due to considerable cross-coupling effects unaccountable by simpler models, e.g., equivalent networks [7]. At the same time, EM analysis may be computationally demanding which poses practical challenges when a large number of simulations are required. This is pertinent to local parameter adjustment [8] but even more to global search procedures [9]-[11] or uncertainty quantification [12]. A typically large number of parameters required to describe complex layouts of miniaturized components is an additional challenge. Furthermore, global optimization is often necessary due to difficulties in identifying reasonable initial designs for local optimization [13,14], which is yet another byproduct of topological complexity of modern microwave structures.

The aforementioned issues hinder the utilization of conventional optimization algorithms in a large number of practical situations. Hence, the extensive research oriented towards improving the computational efficiency of simulation-based design procedures is by no means a surprise. Among the various techniques developed over the recent years, several categories of methods are worth noting. These include surrogate-assisted algorithms involving physics-based models (space mapping [15], response

correction methods [16], feature-based optimization [17]), along with optimization frameworks employing data-driven surrogates (kriging [11], artificial neural networks [18], Gaussian process regression [19], or polynomial chaos expansion [20]). Another approaches comprise gradient-based algorithms accelerated through adjoint sensitivities [21], [22], or implementing sparse sensitivity updates [23], [24], as well as machine learning approaches (most often utilized in the context of global optimization [25]). Each of these techniques exhibit specific advantages but also limitations. Physics-based surrogates, for that matter, feature excellent generalization (i.e., the ability to render reliable predictions about the high-fidelity model outputs using a small number of training samples) yet their construction requires appropriate low-fidelity models. The latter are problem specific, may not be always available, or not sufficiently reliable. In juxtaposition to this, data-driven models are more flexible and easily transferrable between application domains but they are strongly affected by the curse of dimensionality. This is a serious drawback from the point of view of high-frequency design as a typical microwave device outputs are highly nonlinear [26].

The algorithmic means of alleviating the high cost issue outlined in the previous paragraph generally assume that the design process (e.g., parameter tuning) starts from scratch every time it is executed, with the initial design often obtained through theoretical considerations or parameter sweeping. On the other hand, computational savings can be achieved by incorporating the already existing data, e.g., in the form of previous designs obtained for various sets of performance specifications. Design curves are perhaps the earliest and the simplest examples of this sort of approach [27]-[29]. Recently, the employment of the inverse surrogate models has been fostered in this context [30], also in

variable-fidelity simulation setup [31], as well as supplemented by the iterative correction schemes [32]. Regardless of a particular implementation, the employment of already available information seems to be a potentially attractive way of speeding up the design process.

This paper proposes a surrogate-assisted procedure for expediting the design closure of miniaturized microwave passives. The keystone of the presented approach is an incorporation of the existing designs in the form of two kriging interpolation models, one for yielding a reasonable initial design, and the other to provide an estimation of the system response sensitivities. The latter permits a jump-start of the design refinement process, here, implemented within the trust-region gradient search with Jacobian updates based on the rank-one Broyden formula. Comprehensive verification involving two impedance matching transformers demonstrates the efficacy of the framework with the optimized designs rendered at the cost of a few EM analyses of the respective structure. For both circuits, the optimization process is carried out over wide ranges of operating conditions without the necessity of providing any initial point, which shows a quasi-global search capability while employing local optimizers only.

2. Optimization with Design Reusing

In this section, we delineate the proposed framework for accelerated design optimization of microwave passives by design reusing. Our methodology involves exploitation of pre-optimized reference designs in order to develop kriging surrogates for the two following purposes: (i) identification of a good quality initial design, and (ii) expediting the optimization (design refinement) procedure.

2.1. Figures of Interest and Database Designs

The proposed methodology assumes the existence of a database comprising the reference designs optimized for the chosen values of design objectives. The required number of such designs is normally small (e.g., a few). Let X refer to the parameter space of tunable variables of the microwave component under design, and let F represent the objective space of performance figures such as a required operating frequency (or frequencies in the case of multi-band structures), bandwidth, power split ratio (in the case of couplers/dividers) or material parameters (e.g., permittivity or height of the substrate used to realize the structure). The performance figure vector $\boldsymbol{F} = [F_1 \ldots F_N]^T \in F$ represents the aggregated design specifications. The aforementioned reference designs $\boldsymbol{x}_b^{(j)}$, $j = 1, \ldots, p$, are optimized for the objective vectors $\boldsymbol{F}^{(j)} = [F_1^{(j)} \ldots F_N^{(j)}]^T$ by solving

$$\boldsymbol{x}^* = \arg\min_{\boldsymbol{x}} U(\boldsymbol{R}(\boldsymbol{x}), \boldsymbol{F}) \tag{1}$$

where $\boldsymbol{R}(\boldsymbol{x})$ denotes the EM-simulated response of the component, e.g., the scattering parameters versus frequency; $\boldsymbol{x} = [x_1 \ldots x_n]^T \in X$, and U refers to the scalar cost function. For the sake of brevity, the design optimized in the sense of (1) with $\boldsymbol{F}$ being a target vector will be referred to as $U_F(\boldsymbol{F})$. In particular, the jth reference design of the design database will be denoted as $\boldsymbol{x}_b^{(j)} = U_F(\boldsymbol{F}^{(j)})$. The vectors $\boldsymbol{F}^{(j)}$ may be arbitrarily allocated within the objective space F, although uniform distribution is preferred. The space F itself is defined as an N-dimensional interval delimited by the intended ranges of the figures of interest, i.e., $F_{k.\min} \le F_k \le F_{k.\max}$. These ranges determine the region of validity of the proposed framework. The database designs may either be acquired during prior work with the structure in question or pre-optimized especially for the purposes of setting up the optimization procedure. In addition, let the Jacobian matrices of the component

response at $\boldsymbol{x}_b^{(j)}$ be denoted as $\boldsymbol{J}_b^{(j)} = \boldsymbol{J}(\boldsymbol{x}_b^{(j)})$, $j = 1, \ldots, p$. The sensitivity data is normally obtained as an additional outcome of solving (1).

In order to explain the above mentioned concepts, let us consider a filter designed to minimize $|S_{11}|$ within the operating band defined by the center frequency f_0 and the fractional bandwidth B. Hence, we have a two-objective space F: $F_1 = f_0$ and $F_2 = B$. In this case, the following objective function U might be employed $U(\boldsymbol{R}(\boldsymbol{x}),\boldsymbol{F}) = \max\{F_1(1 - F_2/2) \leq f \leq F_1(1 + F_2/2) : |S_{11}(\boldsymbol{x},f)|\}$.

2.2. Kriging Surrogates

In the proposed framework, the two following kriging [33] surrogates are constructed based on the set of database designs:

- s_x: $F \rightarrow X$, configured from the pairs $\{\boldsymbol{F}^{(j)},\boldsymbol{x}_b^{(j)}\}_{j=1,\ldots,p}$;
- $s_J(\cdot)$: $F \rightarrow X \times \ldots \times X$ (m-times Cartesian product of X, with where m refers to the dimension of the component response vector $\boldsymbol{R}(\cdot)$), constructed from the data set $\{\boldsymbol{F}^{(j)},\boldsymbol{J}_b^{(j)}\}_{j=1,\ldots,p}$.

The output of the model $s_x(\boldsymbol{F})$ approximates the design optimized with respect to the performance figure vector $\boldsymbol{F}$. Thus, s_x is an inverse surrogate. The model s_J provides approximation of the component response sensitivities at the design produced by s_x. A graphical illustration of the relationship between the kriging models and the objective space has been shown in Fig. 1.

2.3. Initial Design

The inverse model s_x delivers the best available approximation of the optimum design set $U_F(F)$ that can be obtained based on the reference designs $\boldsymbol{x}_b^{(j)} = U_F(\boldsymbol{F}^{(j)})$, $j = 1, \ldots, p$. In particular, the initial estimate of the design $U_F(\boldsymbol{F}_t)$ optimum with respect to a target vector $\boldsymbol{F}_t \in F$ may be found as

$$\boldsymbol{x}^{(0)} = s_x(\boldsymbol{F}_t) \tag{2}$$

Additionally, an approximation of the Jacobian matrix of the component responses at $\boldsymbol{x}^{(0)}$ is provided by the second surrogate s_J as

$$\boldsymbol{J}^{(0)} = s_J(\boldsymbol{F}_t) \tag{3}$$

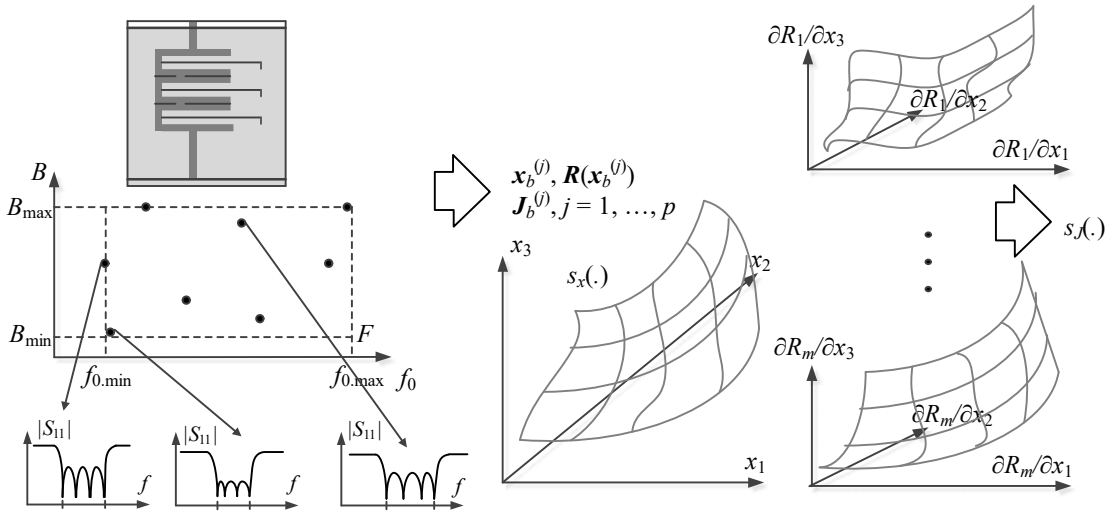

Fig. 1. Graphical illustration of the objective space (delimited by the lower and upper bounds on the center frequency f_0 and the fractional bandwidth B) for a fourth-order bandpass filter presented at the top, along with exemplary filter responses optimized for the selected operating bandwidths that correspond to the objective vectors from the objective space F (left panel). The surrogates s_x and s_J (right panel) are set up with the use of the database designs (black circles) and corresponding filter responses along with their sensitivities.

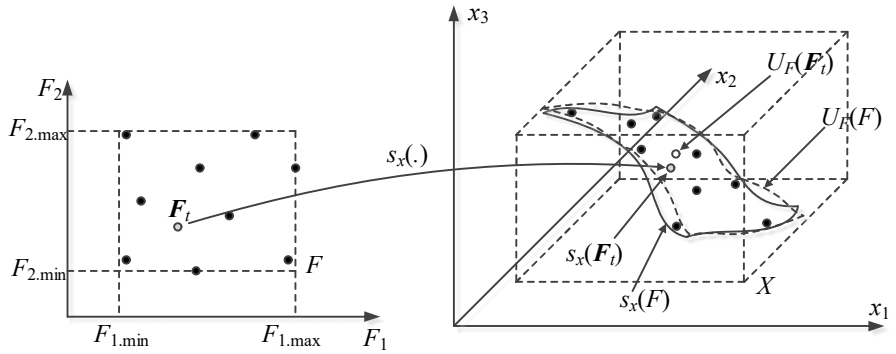

Fig. 2. Conceptual illustration of the image $s_x(F)$ (solid lines) of the objective space F, along with the optimum design manifold $U_F(F)$ (dashed lines). The exemplary initial design $s_x(\boldsymbol{F}_t)$ (gray-shaded circle) corresponds to the target vector $\boldsymbol{F}_t$. The surrogate $s_x(\cdot)$ is constructed based on the reference designs (black circles). The true optimum design $U_F(\boldsymbol{F}_t)$ (white-shaded circle) differs from $s_x(\boldsymbol{F}_t)$ because $s_x(F)$ merely approximates $U_F(F)$.

The above concepts are illustrated graphically in Fig. 2. The initial design $\boldsymbol{x}^{(0)}$, established using (2), is only an approximation of $U_F(\boldsymbol{F}_t)$, and its quality is determined, among others, by the number of the database designs and the nonlinearity of the component response. Hence, it needs to be further refined which is carried out with the use of a trust-region (TR) gradient search algorithm [34].

The TR algorithm is an iterative procedure that produces a series of approximations $\boldsymbol{x}^{(i)}$, $i = 0, 1, \ldots$, to $\boldsymbol{x}^* = U_F(\boldsymbol{F}_t)$ by solving subproblems

$$\boldsymbol{x}^{(i+1)} = \arg\min_{\boldsymbol{x};\, -\boldsymbol{d}^{(i)} \le \boldsymbol{x}-\boldsymbol{x}^{(i)} \le \boldsymbol{d}^{(i)}} U(\boldsymbol{G}^{(i)}(\boldsymbol{x}), \boldsymbol{F}_t) \tag{4}$$

where $G^{(i)}(\boldsymbol{x})$ is a first-order Taylor expansion of $\boldsymbol{R}$

$$\boldsymbol{G}^{(i)}(\boldsymbol{x}) = \boldsymbol{R}(\boldsymbol{x}^{(i)}) + \boldsymbol{J}_{\boldsymbol{R}}(\boldsymbol{x}^{(i)}) \cdot (\boldsymbol{x} - \boldsymbol{x}^{(i)}) \tag{5}$$

Usually, the Jacobian $\boldsymbol{J}_{\boldsymbol{R}}$ is updated in each algorithm iteration through computationally expensive finite differentiation (FD), at the cost of n additional EM simulations of the device at hand. By exploiting the fact that the initial design (2) is typically good, a reduction of the computational overhead associated with solving (4) can be attained

through updating the Jacobian $\boldsymbol{J_R}$ in consecutive iterations with the use of the Broyden formula [34] rather than FD. In addition, in the first iteration, the Jacobian is jump-started with $s_J(\boldsymbol{F}_I)$ yielded by the forward model s_J. As a consequence, the cost of the optimization process is significantly reduced to no more than a few EM analyses of the component under design.

3. Verification Case Studies

In this section, numerical validation of the methodology of Section 2.3 is provided using the three- and four-section impedance matching transformers described by fifteen and twenty geometry parameters, respectively. The results confirm the ability of the proposed framework to deliver high quality designs satisfying assumed target specifications at a low computational cost.

3.1. Benchmark structures

The verification structures are two compact impedance matching transformers shown in Fig. 3(b) and (c). The circuits are composed of compact microstrip resonant cells (CMRCs) shown in Fig. 3(a). Both transformers are implemented on a 0.762-mm-thick Taconic RF35 substrate (ε_r = 3.5). The geometry parameters are presented in Table 1. The three-section transformer has been optimized for various operating bands [f_1 f_2] within the ranges 1.5 GHz $\leq f_1 \leq$ 3.5 GHz, and 4.5 GHz $\leq f_2 \leq$ 6.5 GHz. Here, the optimum design minimizes the maximum of the reflection $|S_{11}|$ within [f_1 f_2]. Whereas in the case of the four-section transformer the region of interest is defined by 1.5 GHz $\leq f_1 \leq$ 3.5 GHz, and 5.5 GHz $\leq f_2 \leq$ 6.5 GHz.

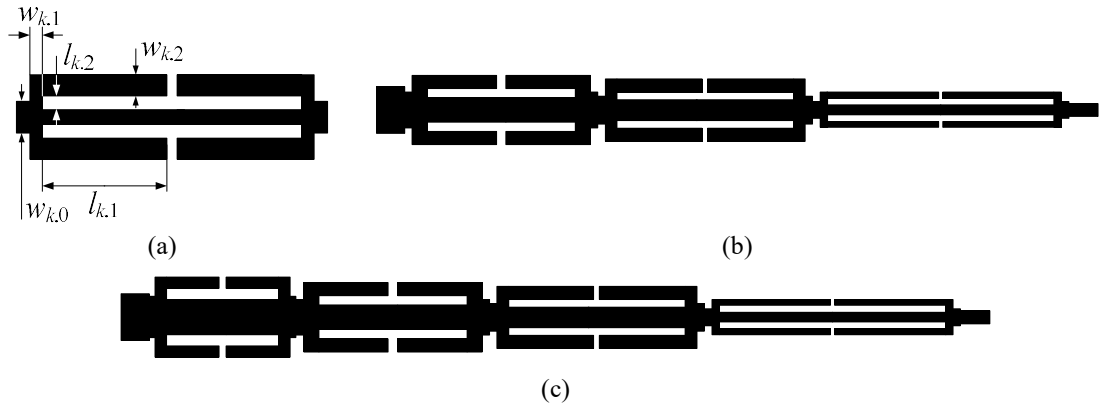

Fig. 3. Verification test cases: (a) CMRC cell, (b) and (c) CMRC-based miniaturized three- and four-section impedance matching transformers, respectively.

Table 1. Geometry Parameters of the Three- and Four Section Impedance Transformers

Circuit	Geometry Parameters
3-section	$[l_{1.1}\ l_{1.2}\ w_{1.1}\ w_{1.2}\ w_{1.0}\ l_{2.1}\ l_{2.2}\ w_{2.1}\ w_{2.2}\ w_{2.0}$ $l_{3.1}\ l_{3.2}\ w_{3.1}\ w_{3.2}\ w_{3.0}]^T$
4-section	$[l_{1.1}\ l_{1.2}\ w_{1.1}\ w_{1.2}\ w_{1.0}\ l_{2.1}\ l_{2.2}\ w_{2.1}\ w_{2.2}\ w_{2.0}$ $l_{3.1}\ l_{3.2}\ w_{3.1}\ w_{3.2}\ w_{3.0}\ l_{4.1}\ l_{4.2}\ w_{4.1}\ w_{4.2}\ w_{4.0}]^T$

In the case of the three-section transformer, five reference designs $\boldsymbol{x}_b^{(j)}$, corresponding to the pairs $\{f_1,f_2\}$: {1.5, 4.5}, {1.5, 6.5}, {2.5, 5.5}, {3.5, 4.5}, and {3.5, 6.5} (frequencies in GHz), have been used. For the four-section transformer, the number of the reference designs was nine, representing the following operational bandwidths: {1.5, 5.5}, {1.5, 6.5}, {1.5, 7.5}, {2.5, 5.5}, {2.5, 6.5}, {2.5, 7.5}, {3.5, 5.5}, {3.5, 6.5}, and {3.5, 7.5} (frequencies in GHz). It should be emphasized that the design optimization tasks are challenging due to a small number of the reference designs but also high dimensionality of the parameter spaces.

Tables 2 and 3 gather the numerical results obtained by optimizing the three- and four-section transformers, respectively, for the target performance vectors selected for

validation purposes. Figures 4 and 5, respectively, show the components responses at the initial designs (obtained using (2)), as well as the final designs yielded by solving (4), (5). The average computational cost of the optimization process does not exceed eight EM simulations of the transformer circuit (in the case of three-section transformer) and for four-section transformer the computational overhead is as low as nine EM simulations.

3.2. Discussion

The initial designs, yielded by the first-level (inverse) surrogate (cf. (2)), are of high quality for all verification cases and for both transformers. Employing TR algorithm (4) and (5) permits further design improvement for the majority of the cases.

Table 2. Optimization Results for Three-Section Impedance Transformer

Test case		1	2	3	4	5	6
Target operating band	f_1 [GHz]	2.0	1.8	2.7	2.7	3.5	2.8
	f_2 [GHz]	5.0	6.0	5.2	5.8	6.0	4.9
Geometry parameters [mm]	$l_{1.1}$	2.94	2.82	2.57	2.42	2.17	2.56
	$l_{1.2}$	0.34	0.15	0.29	0.35	0.33	0.38
	$w_{1.1}$	0.75	0.80	0.79	0.80	0.81	0.76
	$w_{1.2}$	0.51	0.47	0.54	0.55	0.52	0.54
	$w_{1.0}$	1.25	0.86	1.14	0.61	0.76	1.26
	$l_{2.1}$	3.57	3.38	3.42	3.44	3.06	3.33
	$l_{2.2}$	0.35	0.15	0.18	0.23	0.16	0.30
	$w_{2.1}$	0.54	0.68	0.52	0.66	0.62	0.52
	$w_{2.2}$	0.27	0.15	0.32	0.15	0.24	0.34
	$w_{2.0}$	0.83	0.32	0.99	0.36	0.81	1.03
	$l_{3.1}$	4.07	3.94	3.80	3.58	3.35	3.85
	$l_{3.2}$	0.22	0.15	0.15	0.15	0.14	0.18
	$w_{3.1}$	0.35	0.46	0.34	0.37	0.37	0.33
	$w_{3.2}$	0.20	0.15	0.17	0.15	0.15	0.20
	$w_{3.0}$	0.59	1.00	0.66	0.60	0.55	0.51

For the three-section transformer, in one occurrence (cf. Fig. 4(e)), the initial design characterized by a very low in-band reflection has not been altered by (4). This was due to the presence of numerical noise in EM simulations results that hinders the gradient search based on approximated sensitivity data. In the case of four-section transformer, the initial designs produced by (2) are of good quality for all considered cases. Also, for all target operating bands, the gradient-based refinement (4) brings visible improvement.

Table 3. Optimization Results for Four-Section Impedance Transformer

Test case		1	2	3	4	5	6
Target operating band	f_1 [GHz]	1.8	2.0	2.2	2.2	2.4	2.8
	f_2 [GHz]	5.8	7.5	5.8	6.4	7.0	6.3
Geometry parameters [mm]	$l_{1.1}$	3.14	2.30	2.70	2.69	2.35	2.31
	$l_{1.2}$	0.12	0.24	0.10	0.15	0.25	0.14
	$w_{1.1}$	0.99	0.96	1.00	1.00	0.98	0.98
	$w_{1.2}$	0.42	0.34	0.43	0.40	0.38	0.46
	$w_{1.0}$	0.32	0.46	0.45	0.63	0.50	0.81
	$l_{2.1}$	3.84	3.27	3.70	3.61	3.36	3.53
	$l_{2.2}$	0.19	0.13	0.18	0.17	0.16	0.17
	$w_{2.1}$	0.79	0.86	0.82	0.85	0.86	0.88
	$w_{2.2}$	0.15	0.10	0.15	0.13	0.13	0.11
	$w_{2.0}$	0.20	0.18	0.17	0.20	0.18	0.46
	$l_{3.1}$	4.18	3.24	3.99	3.74	3.38	3.53
	$l_{3.2}$	0.13	0.10	0.10	0.10	0.10	0.10
	$w_{3.1}$	0.43	0.47	0.42	0.42	0.45	0.40
	$w_{3.2}$	0.11	0.10	0.10	0.10	0.10	0.10
	$w_{3.0}$	0.22	0.12	0.36	0.38	0.17	0.56
	$l_{4.1}$	3.54	2.61	3.25	3.05	2.70	2.78
	$l_{4.2}$	0.14	0.15	0.15	0.14	0.13	0.13
	$w_{4.1}$	0.17	0.17	0.15	0.16	0.16	0.13
	$w_{4.2}$	0.10	0.13	0.10	0.10	0.13	0.10
	$w_{4.0}$	1.45	1.30	1.31	1.37	1.27	1.39

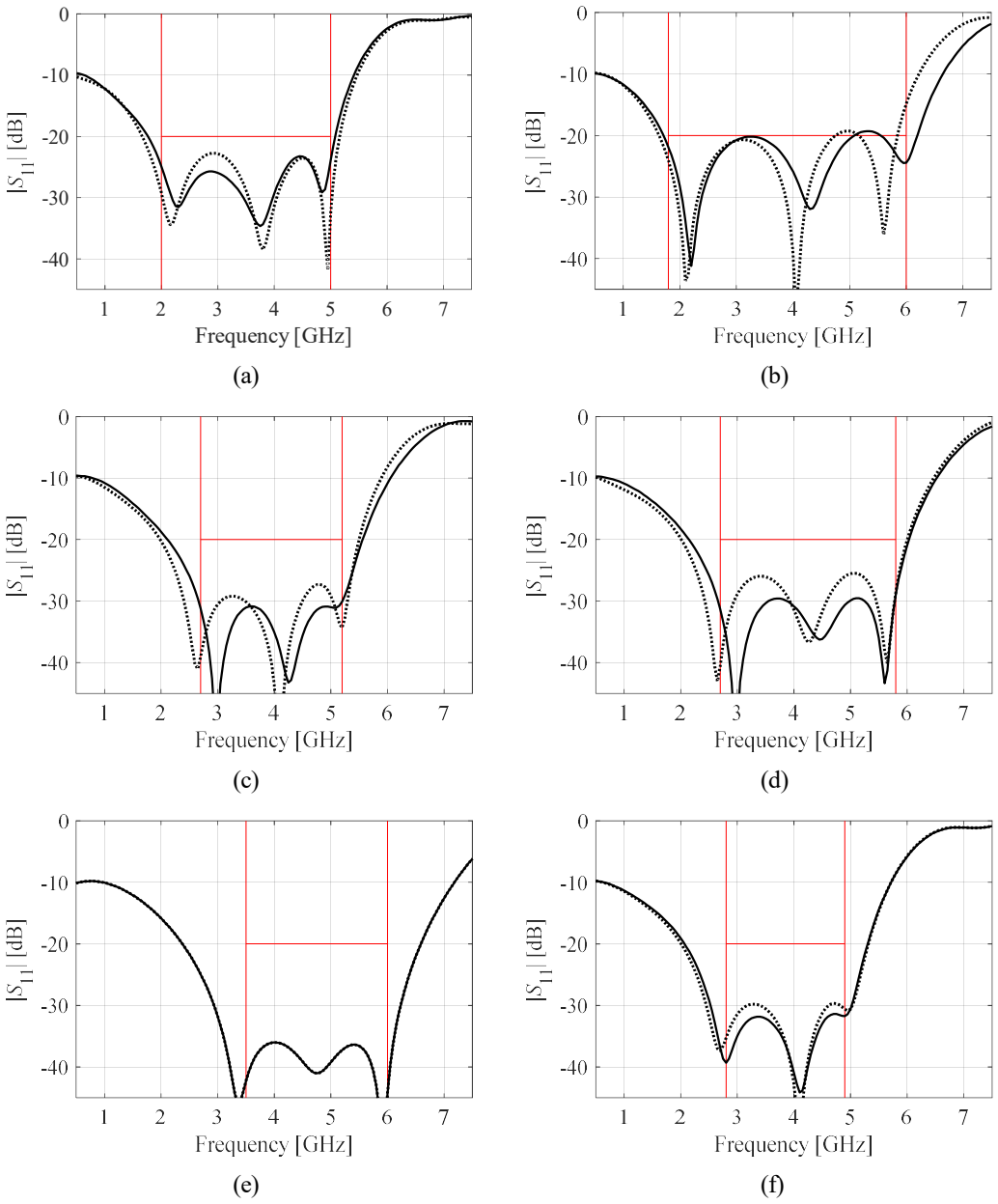

Fig. 4. The responses of three-section impedance matching transformer: initial design found using (2) (····) and the final design obtained using (4), (5) (—). Shown are designs corresponding to the target vectors of Table 2: (a) f_1 = 2.0 GHz, f_2 = 5.0 GHz, (b) f_1 = 1.8 GHz, f_2 = 6.0 GHz, (c) f_1 = 2.7 GHz, f_2 = 5.2 GHz, (d) f_1 = 2.7 GHz, f_2 = 5.8 GHz, (e) f_1 = 3.5 GHz, f_2 = 6.0 GHz, (f) f_1 = 2.8 GHz, f_2 = 4.9 GHz. Red lines indicate intended bandwidths as well as performance specifications.

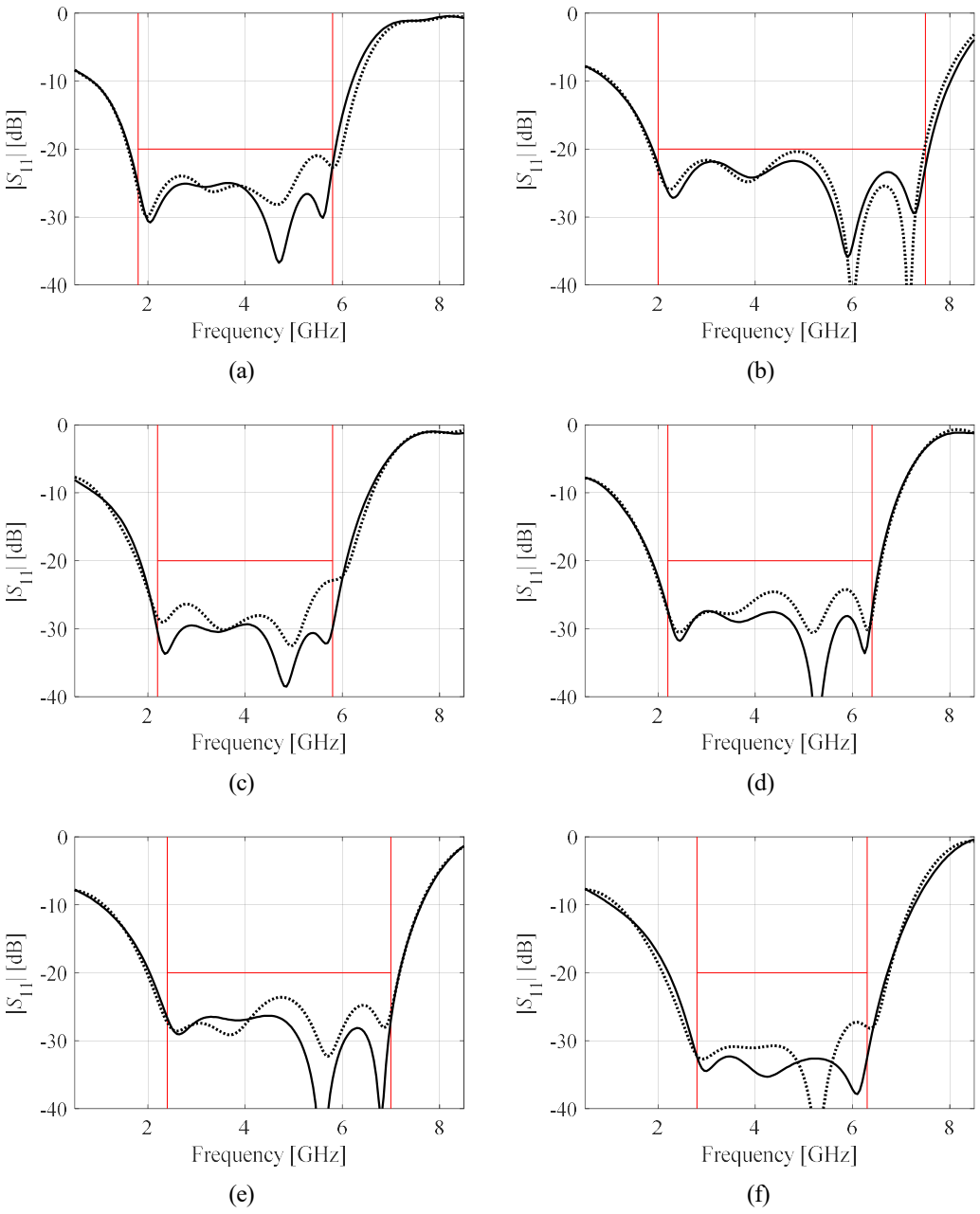

Fig. 5. The responses of four-section impedance matching transformer obtained with the optimization framework set up with nine reference designs: initial design found using (2) (····) and the final design obtained using (4), (5) (—). Shown are designs corresponding to the target vectors of Table 3: (a) f_1 = 1.8 GHz, f_2 = 5.8 GHz, (b) f_1 = 2.0 GHz, f_2 = 7.5 GHz, (c) f_1 = 2.2 GHz, f_2 = 5.8 GHz, (d) f_1 = 2.2 GHz, f_2 = 6.4 GHz, (e) f_1 = 2.4 GHz, f_2 = 7.0 GHz, (f) f_1 = 2.8 GHz, f_2 = 6.3 GHz. Red lines indicate intended bandwidths as well as performance specifications.

In order to further demonstrate the robustness of the proposed framework, optimization of the four-section transformer has been repeated using only five reference designs, corresponding to the following bandwidths: {1.5, 5.5}, {1.5, 7.5}, {2.5, 6.5}, {3.5, 5.5}, and {3.5, 7.5} (frequency in GHz). Figure 6 shows the transformer responses at the initial and optimized designs. The average computational cost of the parameter tuning process is similar to the previous case (i.e., around eight EM simulations), and both the initial and final designs are of good quality. Table 4 gathers the maximum in-band reflection levels for both situations (nine and five reference designs). The average reflection level (over the considered target bandwidth) is only lower by 0.3 dB in favor of the nine-reference-design setup.

3. Conclusions

The paper proposed a simple yet efficient framework for expedited design optimization of miniaturized microwave components. Our methodology exploits the pre-existing designs optimized for the selected values of performance figures pertinent to the component at hand, as well as two kriging surrogate models.

Table 4. Design Quality Comparison for Four-Section Impedance Transformer: Optimization Framework with Nine versus Five Reference Designs

Test case		1	2	3	4	5	6
Target operating band	f_1 [GHz]	1.8	2.0	2.2	2.2	2.4	2.8
	f_2 [GHz]	5.8	7.5	5.8	6.4	7.0	6.3
Maximum in-band reflection (nine reference designs)		–22.4 dB	–21.7 dB	–29.3 dB	–27.3 dB	–26.3 dB	–32.3 dB
Maximum in-band reflection (five reference designs)		–23.4 dB	–23.1 dB	–25.1 dB	–27.5 dB	–24.5 dB	–33.8 dB

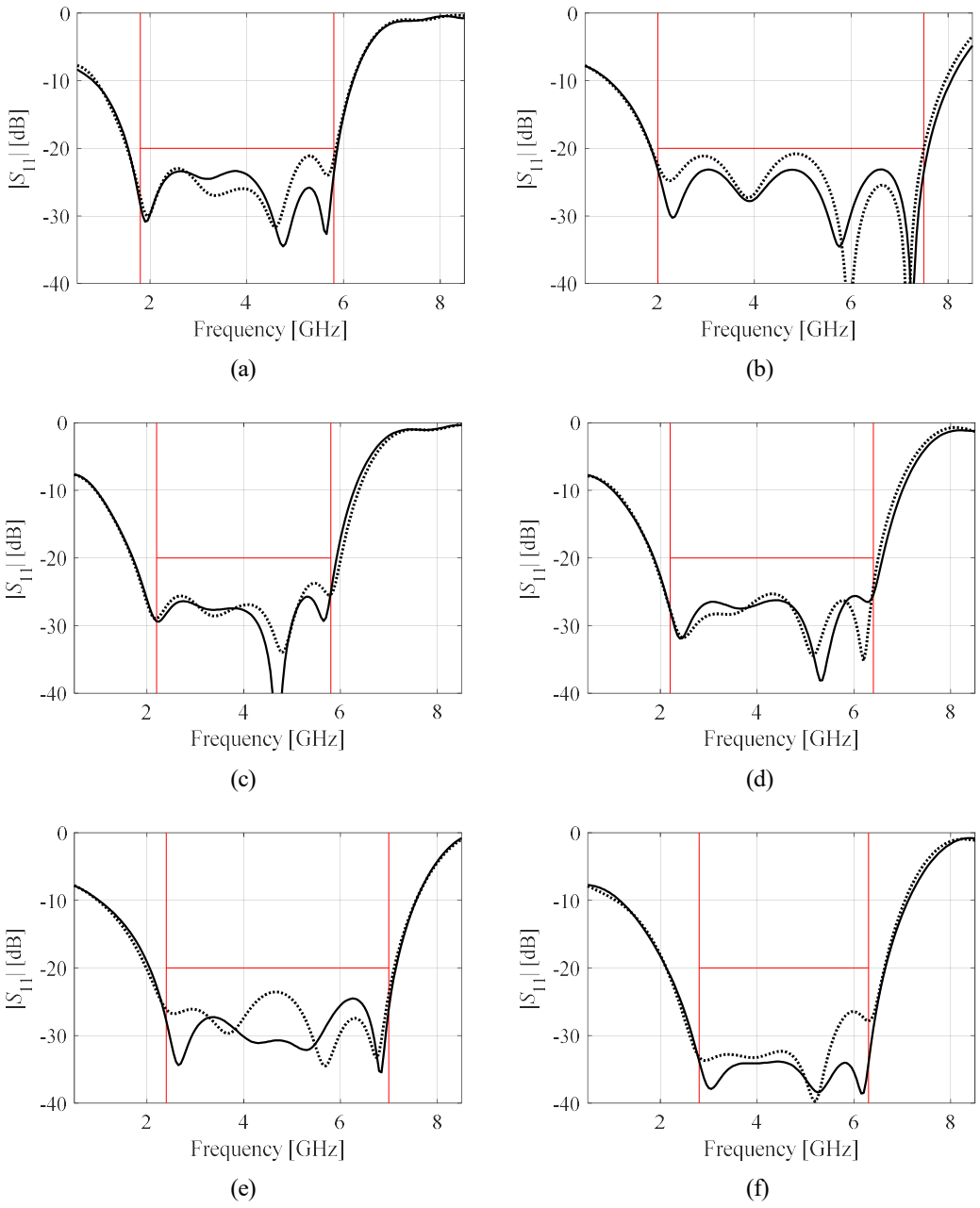

Fig. 6. The responses of four-section impedance matching transformer obtained with the optimization framework set up with five reference designs: initial design found using (2) (····) and the final design obtained using (4), (5) (—). Shown are designs corresponding to the target vectors of Table 3: (a) f_1 = 1.8 GHz, f_2 = 5.8 GHz, (b) f_1 = 2.0 GHz, f_2 = 7.5 GHz, (c) f_1 = 2.2 GHz, f_2 = 5.8 GHz, (d) f_1 = 2.2 GHz, f_2 = 6.4 GHz, (e) f_1 = 2.4 GHz, f_2 = 7.0 GHz, (f) f_1 = 2.8 GHz, f_2 = 6.3 GHz. Red lines indicate intended bandwidths as well as performance specifications.

The first model yields a reasonably good initial design corresponding to the target performance figures, whereas the second model delivers an approximation of the Jacobian matrix of the component response, utilized to jump-start the design refinement process. The optimization procedure is further accelerated by replacing costly finite-differentiation-based Jacobian updates with the Broyden formula.

The proposed framework has been validated using two impedance matching transformers described by large numbers of geometry parameters (fifteen and twenty, respectively), optimized within wide ranges of operating bandwidths. The obtained results demonstrate the capability of the presented approach of yielding high-quality designs at the computational cost as low as a few EM simulations of the structure at hand. Additional experiments conducted for the four-section transformer corroborate the robustness of our methodology as being capable of yielding good results even if the number of pre-existing designs is severely limited. At the same time, because no user-provided initial design is necessary, the framework can be considered a quasi-global procedure (within the range of validity in terms of the considered performance figures).

The proposed approach can be a suitable tool for expediting the parameter tuning procedures especially whenever a certain number of designs are already available for a given structure, or the expected multiple use of the framework justifies the initial effort associated with generating the reference designs required to set up the kriging surrogates.

Acknowledgement

The authors would like to thank Dassault Systemes, France, for making CST Microwave Studio available. This work is partially supported by the Icelandic Centre for

Research (RANNIS) Grant 174573051 and by National Science Centre of Poland Grant 2018/31/B/ST7/02369.

References

[1] Mayani MG, Asadi S, Pirhadi A, Mahani SM. Design and analysis of a super compact wide-band bandpass filter based on metamaterial resonators. AEU – Int J Electr Comm 2018; 97:79–84. https://doi.org/10.1016/j.aeue.2018.10.010.

[2] Song L, He L. Research on dual-polarized circular waveguide antenna fed by L-shaped probes. AEU – Int J Electr Comm 2018; 83:156–167. https://doi.org/10.1016/j.aeue.2017.08.023.

[3] Melgarejo JC, Ossorio J, Cogollos S, Guglielmi M, Boria VE, Bandler JW. On space mapping techniques for microwave filter tuning. IEEE Trans Microwave Theory Techn 2019; https://doi.org/10.1109/TMTT.2019.2944361.

[4] Kurgan P, Koziel S. Selection of circuit geometry for miniaturized microwave components based on concurrent optimization of performance and layout area. AEU – Int J Electr Comm 2019; 108, 2019; 287–294. https://doi.org/10.1016/j.aeue.2019.06.009.

[5] Koziel S, Pietrenko-Dabrowska A. Reduced-cost electromagnetic-driven optimisation of antenna structures by means of trust-region gradient-search with sparse Jacobian updates. IET Microw Ant Propag 2019; 13:1646–1652. https://doi.org/10.1049/iet-map.2018.5879.

[6] Merenda M, Felini C, Della Corte FG. A monolithic multisensor microchip with complete on-chip RF front-end. Sensors 2018; 18:110. https://doi.org/10.3390/s18010110.

[7] Koziel S, Kurgan P. Rapid design of miniaturized branch-line couplers through concurrent cell optimization and surrogate-assisted fine-tuning. IET Microw Ant Propag 2015; 957–963. https://doi.org/10.1049/iet-map.2014.0600.

[8] Bekasiewicz A, Koziel S. Reliable multistage optimization of antennas for multiple performance figures in highly dimensional parameter spaces. IEEE Ant Wireless Propag Lett 2019; 18:1522–1526. https://doi.org/10.1109/LAWP.2019.2921610.

[9] Ustun D, Akdagli A. Design of band–notched UWB antenna using a hybrid optimization based on ABC and DE algorithms. AEU – Int J Electr Comm 2018; 87:10–21. https://doi.org/10.1016/j.aeue.2018.02.001.

[10] Torun HM, Swaminathan M. High-dimensional global optimization method for high-frequency electronic design. IEEE Trans Microwave Theory Techn 2019; 67: 2128–2142. https://doi.org/10.1109/TMTT.2019.2915298.

[11] Dong J, Li Q, Deng L. Fast multi-objective optimization of multi-parameter antenna structures based on improved MOEA/D with surrogate-assisted model.

AEU – Int J Electr Comm 2017; 72:192–199. https://doi.org/10.1016/j.aeue.2016.12.007.

[12] Prasad AK, Ahadi M, Roy S. Multidimensional uncertainty quantification of microwave/RF networks using linear regression and optimal design of experiments. IEEE Trans Microwave Theory Techn 2016; 64:2433–2446. https://doi.org/10.1109/TMTT.2016.2584608.

[13] Koziel S, Ogurtsov S. Antenna design by simulation-driven optimization. Berlin: Springer; 2014.

[14] Aghayari H, Nourinia J, Ghobadi C, Mohammadi B. Realization of dielectric loaded waveguide filter with substrate integrated waveguide technique based on incorporation of two substrates with different relative permittivity, AEU – Int J Electr Comm 2018; 86:17–24. https://doi.org/10.1016/j.aeue.2018.01.008.

[15] Feng F, Zhang J, Zhang W, Zhao Z, Jin J, Zhang Q. Coarse- and fine-mesh space mapping for EM optimization incorporating mesh deformation. IEEE Microwave Wireless Comp Lett 2019; 29:510–512. https://doi.org/10.1109/LMWC.2019.2927113.

[16] Koziel S, Bekasiewicz A. Pareto-ranking bisection algorithm for expedited multiobjective optimization of antenna structures. IEEE Ant Wireless Propag Lett 2017; 16:1488–1491. https://doi.org/10.1109/LAWP.2016.2646842.

[17] Koziel S, Bekasiewicz A. Fast simulation-driven feature-based design optimization of compact dual-band microstrip branch-line coupler. Int J RF and Microwave Comp Aid Eng 2016; 26:13–20. https://doi.org/10.1002/mmce.20923.

[18] Jamshidi M, Lalbakhsh A, Mohamadzade B, Siahkamari H, Hadi Mousavi SM. A novel neural-based approach for design of microstrip filters. AEU – Int J Electr Comm 2019; 110:152847. https://doi.org/10.1016/j.aeue.2019.152847.

[19] Chen Y, Tian Y, Qiang Z, Xu L. Optimisation of reflection coefficient of microstrip antennas based on KBNN exploiting GPR model. IET Microwaves Ant Propag 2018; 12:602–606. https://doi.org/10.1049/iet-map.2017.0282.

[20] Zhang J, Feng F, Na W, Yan S, Zhang Q. Parallel space-mapping based yield-driven EM optimization incorporating trust region algorithm and polynomial chaos expansion. IEEE Access 2019; 7:143673–143683. https://doi.org/10.1109/ACCESS.2019.2944415.

[21] Karatzidis DI, Yioultsis TV, Tsiboukis TD. Gradient-based adjoint-variable optimization of broadband microstrip antennas with mixed-order prism macroelements. AEU – Int J Electr Comm 2008; 62:401–412. https://doi.org/10.1016/j.aeue.2007.05.011.

[22] Bekasiewicz A, Koziel S. Accelerated geometry optimization of compact impedance matching transformers using decomposition and adjoint sensitivities. Int J Numer Model 2016; 29: 1140– 1148. https://doi.org/10.1002/jnm.2173.

[23] Pietrenko-Dabrowska A, Koziel S. Numerically efficient algorithm for compact microwave device optimization with flexible sensitivity updating scheme. Int J RF Microw Comput Aided Eng 2019; 29:e21714. https://doi.org/10.1002/mmce.21714.

[24] Koziel S, Pietrenko-Dabrowska A. Reduced-cost electromagnetic-driven optimisation of antenna structures by means of trust-region gradient-search with sparse Jacobian updates. IET Microwaves Ant Propag 2019; 13:1646–1652. https://doi.org/10.1049/iet-map.2018.5879.

[25] Goudos S. Design of microwave broadband absorbers using a self-adaptive differential evolution algorithm. Int J RF and Microwave Comp Aid Eng 2009; 19:364–372. https://doi.org/10.1002/mmce.20357.

[26] Goudos S. Microwave systems and applications. London: IntechOpen; 2017.

[27] Mahon SJ, Skellern DJ. Procedure for inverse modelling of GaAs/AlGaAs HEMT structures from DC I/V characteristic curves. Electr Lett 1991; 27:81–82. https://doi.org/10.1049/el:19910052.

[28] Swanson DG. Narrow-band microwave filter design. IEEE Microwave Magazine 2007; 8:105–114. https://doi.org/10.1109/MMM.2007.904724.

[29] Della Corte FG, Merenda M, Bellizzi GG, Isernia T, Carotenuto R. Temperature effects on the efficiency of dickson charge pumps for radio frequency energy harvesting IEEE Access 2018, 6(8502044):65729-65736. https://doi.org/10.1109/ACCESS.2018.2876920.

[30] Koziel S, Bekasiewicz A. Expedited geometry scaling of compact microwave passives by means of inverse surrogate modeling. IEEE Trans Microwave Theory Tech. 2015; 63:4019–4026. https://doi.org/10.1109/TMTT.2015.2490662.

[31] Koziel S, Bekasiewicz A. Rapid dimension scaling of dual-band antennas using variable-fidelity EM models and inverse surrogates. J Electromagn Waves App. 2017; 31:297–308. https://doi.org/10.1080/09205071.2016.1276861.

[32] Koziel S, Bekasiewicz A. Low-cost and reliable geometry scaling of compact microstrip couplers with respect to operating frequency, power split ratio, and dielectric substrate parameters. IET Microwaves Ant Propag. 2018; 12:1508–1513. https://doi.org/10.1049/iet-map.2017.1166.

[33] Simpson TW, Peplinski JD, Koch PN, Allen JK. Metamodels for computer-based engineering design: survey and recommendations. Eng Computers 2001; 17:129–150. https://doi.org/ 10.1007/PL00007198.

[34] Conn AR, Gould NIM, Toint PL. Trust region methods. Philadelphia: Society for Industrial and Applied Mathematics; 2000.